THE ARCHIVE OF MECHANICAL ENGINEERING

VOL. LVI 2009 Number 1

DOI: 10.24425/ame.2009.132089

Key words: piston rings, gasdynamics, hydrodynamics, surface roughness, experimental verification

ANDRZEJ WOLFF *

EXPERIMENTAL VERIFICATION OF THE MODEL OF PISTON RING PACK OPERATION OF AN INTERNAL COMBUSTION ENGINE

In the paper, the author analyses a model of a ring pack motion on an oil film. The local thickness of the oil film can be compared to the height of the combined surface roughness of a cylinder liner and piston rings. Equations describing the mixed lubrication problem based on the empirical mathematical model formulated in works by Patir, Cheng [6, 7] and Greenwood, Tripp [3] have been combined [13] and used in this paper. A model of a gas flow through the labyrinth seal of piston rings has been developed [14,16]. In addition, models of ring twist effects and axial ring motion in piston grooves have been applied [15,16].

In contrast to the previous papers of the author, an experimental verification of the main parts of developed mathematical model and software has been presented. A relatively good compatibility between the experimental measurements and calculated results has been achieved.

1. Introduction

Piston rings are important part of internal combustion engines. Commonly, a set of piston rings is used to form a dynamic gas seal between the piston and cylinder wall. The sliding motion of the piston forms a thin oil film between the ring land and cylinder wall, which lubricates the sliding components [4,9,12]. The hydrodynamic force generated by this thin oil film is opposed by a combination of the gas pressure acting on the back side of each ring and the ring stiffness. Due to the dynamic nature of these forces, each individual ring is periodically compressed and expanded as the piston runs through its cycle. The problem of studying this interaction is further complicated by the high temperatures involved, as these result in low oil viscosity and subsequently very low oil film thickness. The oil film

* *Warsaw University of Technology, Faculty of Transport, ul. Koszykowa 75, 00-662 Warsaw, Poland; E-mail: wolff@it.pw.edu.pl*

is typically thick enough to expect the existence of mixed lubrication, so this phenomenon should also be taken into account [3,6,7,13]. Numerical simulation of the processes which take place in a typical piston ring pack operation is important from practical point of view.

In the second part of the paper, an experimental verification of the main parts of developed mathematical model and software has been presented. A relatively good compatibility between the experimental measurements and calculated results has been achieved.

2. Modelling of piston ring pack operation

A combined model of piston rings operation consists of two main models: a) model of gas flow through the labyrinth seal: piston-rings-cylinder, b) model of oil flow in the lubrication gap between the ring and cylinder liner. The two mentioned models are coupled. In addition, the following mechanical phenomena exist: a contact of rough surfaces, an axial movement of rings within piston grooves and an elastic torsional deformation of piston rings.

2.1. Model of gas flow through the labyrinth seal of piston rings

The applied physical models of labyrinth seals piston-rings-cylinder liner [14, 16] are presented in Figs. 1a and 1b, respectively for four- and two-stroke engine.

These models consist of several gas volume regions (V_1, V_2, ...), which are connected by orifices with cross-section areas A_1, A_2, ... (Figs. 1a, 1b). The volumes V_3, V_5, ... correspond to volumes among the piston rings, while volumes V_2, V_4, ... correspond to groove volumes behind rings.

In the case of two-lips oil ring of a four-stroke engine (Fig. 1a), it was assumed that no pressure difference exists across that type of ring – full ventilation.

It was also assumed that the gas flow through orifices is isentropic (depending on pressure ratio – subsonic or sonic). The heat transfer between gas volume regions and surrounding walls was taken into account.

In addition, the mathematical description takes into account the changes of defined gas volume regions and cross-section areas between the rings and piston grooves (due to axial movement of the rings) [14, 16].

The mathematical model of these phenomena applies equations of the following fundamental physical laws (here given for a chosen gas volume region *Vol*):

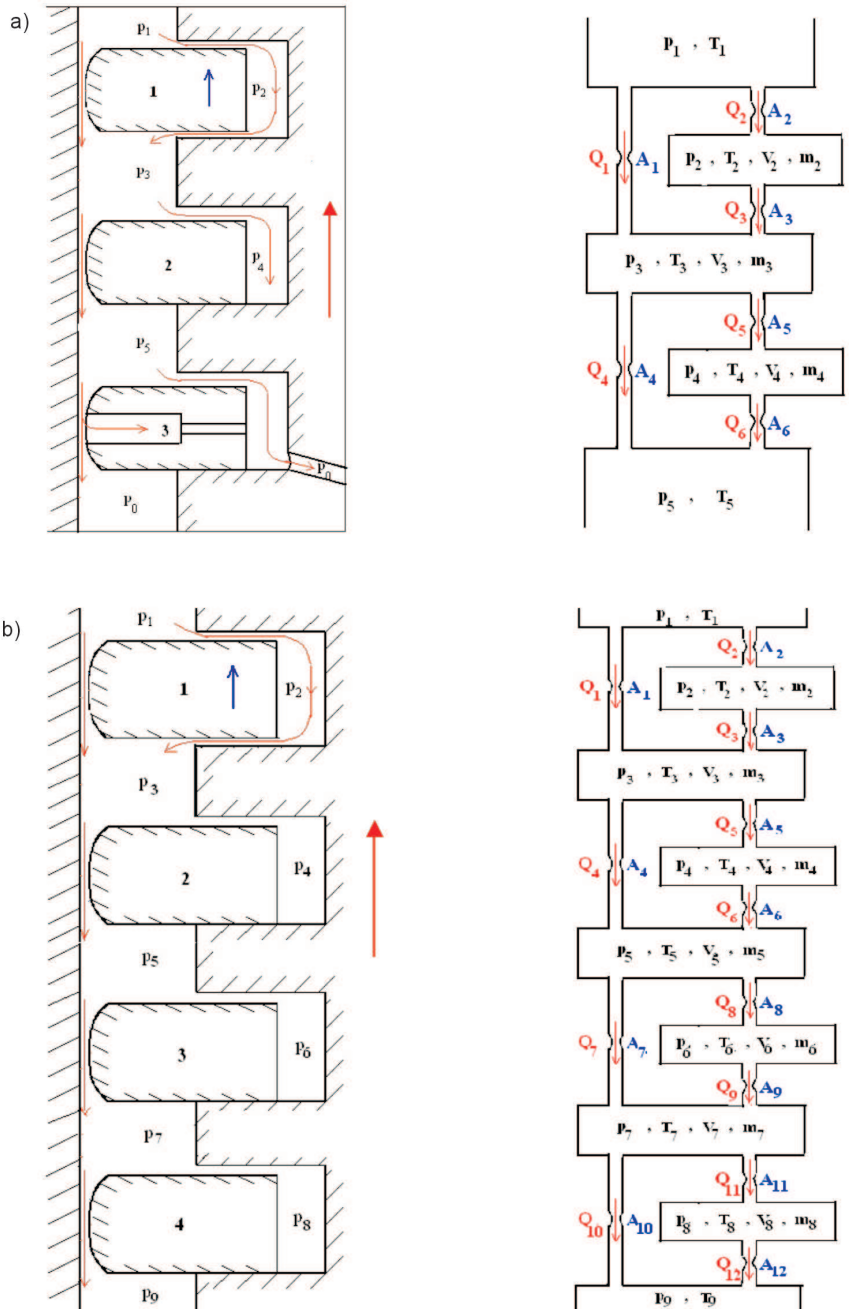

Fig. 1. Scheme of gas flows through the labyrinth system: piston rings – ring grooves – cylinder liner and applied physical models for packs of: a) three piston rings of four-stroke engine, b) four piston rings of two-stroke engine

Equation of mass balance:

$$dm_{Vol} = \sum_i dm_{In_i} - \sum_j dm_{Out_j} \tag{1}$$

Equation of energy balance:

$$\sum_i dm_{In_i} \cdot i_{In_i} - \sum_j dm_{Out_j} \cdot i_{Out_j} - \delta Q_{Wall} = d\left(m_{Vol} \cdot u_{Vol}\right) + p_{Vol} \cdot dV_{Vol} \tag{2}$$

Gas state equation in a differential form:

$$dT_{Vol} = T_{Vol} \cdot \left(\frac{dp_{Vol}}{p_{Vol}} + \frac{dV_{Vol}}{V_{Vol}} - \frac{dm_{Vol}}{m_{Vol}} \right) \tag{3}$$

where: ***m*** – gas mass, ***p*** – gas pressure, ***T*** – gas temperature, ***u*** – internal gas energy, ***i*** – gas enthalpy, ***Q*** – heat transferred through cylinder walls: Index: ***In*** – gas inflow, ***Out*** – gas outflow, ***i*** – number of inflow channel, ***j*** – number of outflow channel, ***Vol*** – analysed gas volume.

Then the final form of these equations was formulated.

2.2. Model of oil flow in a gap (with rough surfaces) between the ring and cylinder

Two main cases of oil flow in the system piston ring – cylinder liner are presented in Fig. 2.

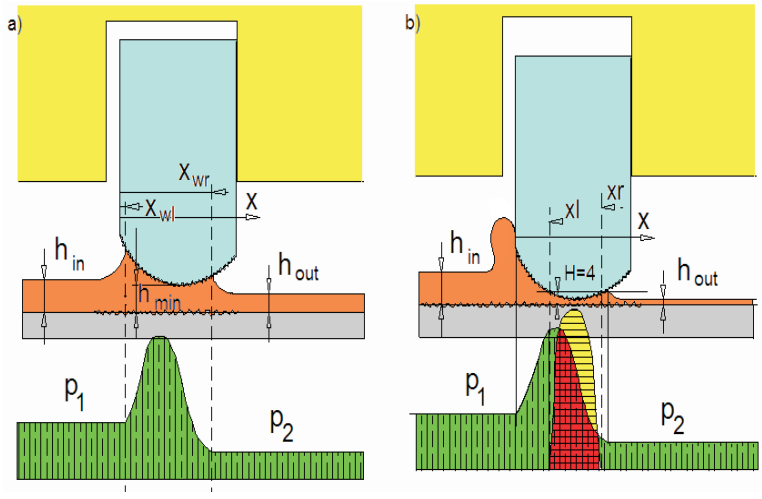

Fig. 2. Flow parameters in the gap between the ring face and cylinder liner in the case of: a) full and b) mixed lubrication

A one dimensional form of the average Reynolds equation developed by Patir and Cheng [6, 7] has been used to calculate hydrodynamic forces in the case of rough gap surfaces. This equation is applicable to any general roughness structure and takes the following form:

$$\frac{\partial}{\partial x}\left(\phi_x \frac{h^3}{12\mu}\frac{d\,\bar{p}}{d\,x}\right) = \frac{u}{2}\frac{d\bar{h}_T}{dx} + \frac{u}{2}\sigma\frac{d\phi_S}{dx} + \frac{d\bar{h}_T}{dt} \tag{4}$$

where: $\boldsymbol{t}$ – time; $\boldsymbol{x}$ – coordinate along cylinder liner; $\boldsymbol{h}$ – nominal oil film thickness; $\boldsymbol{h_T}$ – average separation; $\boldsymbol{p}$ – hydrodynamic pressure; $\boldsymbol{u}$ – axial piston velocity; μ – oil dynamic viscosity; $\boldsymbol{v=\partial h/\partial t}$ – radial piston velocity, $\boldsymbol{\sigma}$ – composite root – mean- square roughness of both mating surfaces.

The significance and mathematical description of empirical coefficients $\boldsymbol{\phi_x}$, $\boldsymbol{\phi_S}$ and boundary conditions of equation (4) are presented in [6, 7] and also in [13].

The effects of interacting asperities of piston ring and cylinder liner surfaces were modelled using the mathematical model developed by Greenwood and Tripp [3], which was precisely described in the publication [13] of the author of this article.

2.3. Model of ring's torsional deformation and ring's axial movement in a piston groove

Fig. 3 shows a scheme of forces acting on piston rings: a) two lip ring, across which no gas pressure drop exists, b) one lip ring.

Equation of the balance of radial forces has the following form:

$$\Sigma F_r = F_h + W_A + F_{yg\,i+1} + F_{yg\,i} - F_{spr} - F_{gas} = 0 \tag{5}$$

where: $\boldsymbol{F_h}$ – hydrodynamic normal force, $\boldsymbol{W_A}$ – elastic direct rough surface contact normal force, $\boldsymbol{F_{spr}}$ – ring spring force, $\boldsymbol{F_{gas}}$ – back ring gas force, $\boldsymbol{F_{ygi+1}}$ – trailing edge gas force, $\boldsymbol{F_{ygi}}$ – leading edge gas force.

The equation of balance of axial forces has the following form:

$$\Sigma F_x = R_x - F_{fri} - F_{WA} + F_{g_{i+1}} - F_{g_i} - \frac{m}{c_{imc}}(g + b_k) = 0 \tag{6}$$

where: $\boldsymbol{R_x}$ – groove reaction force, $\boldsymbol{F_{fri}}$ – viscous friction force, $\boldsymbol{F_{WA}}$ – contact friction force, $\boldsymbol{F_{gi+1}}$ – trailing side gas force, $\boldsymbol{F_{gi}}$ – leading side gas force, $\boldsymbol{m}$ – ring mass, $\boldsymbol{g}$ – gravitational acceleration, $\boldsymbol{b_k}$ – piston acceleration, $\boldsymbol{c_{imc}}$ – ring circumference.

Using this equation, one can calculate the reaction force $\boldsymbol{R_x}$ between the ring and ring-groove. If the sign of this force changes, the axial movement

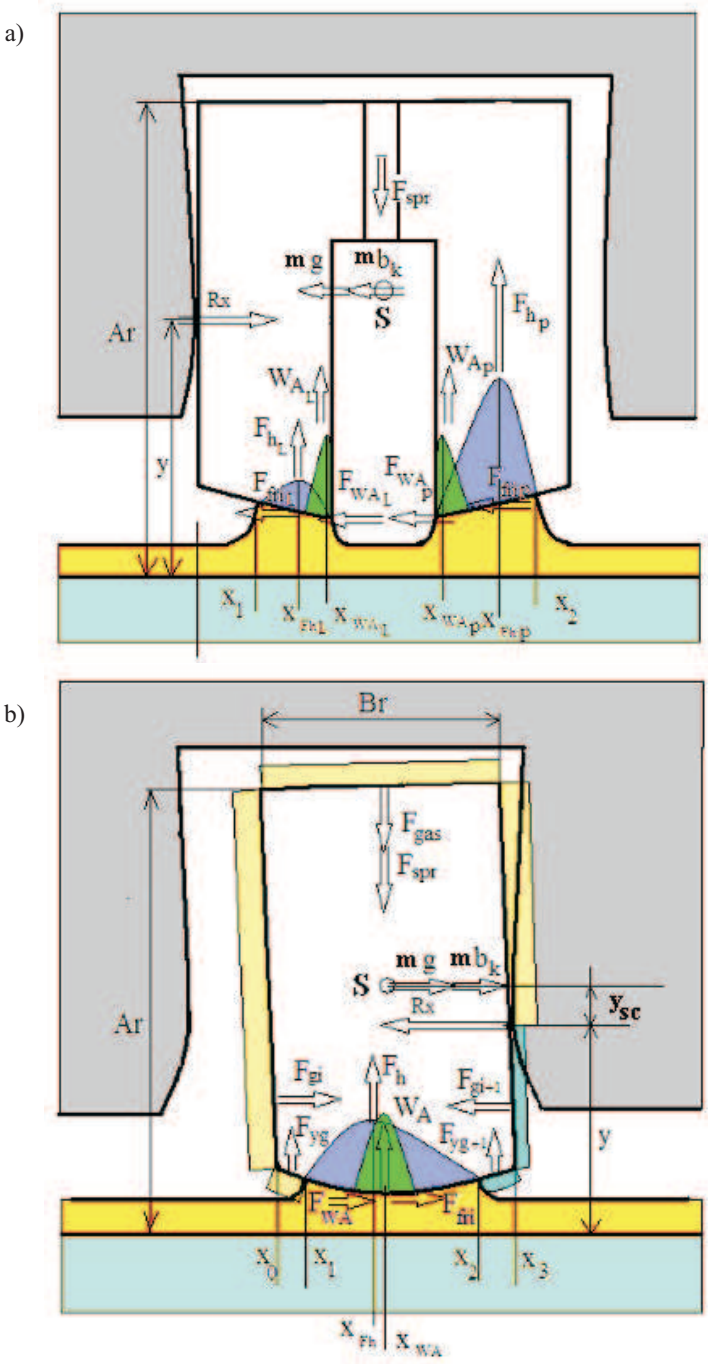

Fig. 3. Scheme and definitions of forces acting on piston rings with regard to twist angles: a) oil ring with two lips, b) compression or scraper ring as a single lip ring

of the ring in the ring-groove begins. In this case, the value of the reaction force $\boldsymbol{R}_x = 0$ and the axial movement of the ring relative to the piston groove can be described by the following differential equation:

$$\frac{m}{c_{imc}}\frac{d^2x_r}{dt^2} = -F_{fri} - F_{WA} + F_{g_{i+1}} - F_{g_i} - \frac{mg}{c_{imc}} \tag{7}$$

The ring movement is finished if the ring reaches the opposite side of the ring-groove.

The twist around the centre of gravity of the ring cross-section (point S in Fig. 3) can be described by the following moments balance equation (8):

$$\begin{aligned}\Sigma M_S = {} & F_h\left(x_S - x_{F_h}\right) + W_A\left(x_S - x_{W_A}\right) - \left(F_{fri} + F_{WA}\right)\frac{A_r}{2} + \\ & + \left(F_{g_{i+1}} - F_{g_i}\right)\left(\frac{y}{2} + y_{sc}\right) + R_x \cdot y_{sc} - K \cdot \theta = 0\end{aligned} \tag{8}$$

Predicting the ring torsional stiffness $\boldsymbol{K}$ [13] and using the moments balance equation (8), one can calculate the ring twist angle $\boldsymbol{\theta}$.

3. Experimental verification of the model

3.1. Preliminary evaluation of developed model and computer code

The general properties of the developed model and computer programme concerning hydrodynamics and oil flow were verified for chosen calculation examples. It was carried out by a comparison of calculation results of an own programme *STOPF* with the results of programme *LUB* that was used by the marine engine designing centre *Wärtsilä* (in Winterthur in Switzerland) several years ago. This work was done during one of many research periods of the author at mentioned company.

As an important case the hydrodynamic system: single scraper ring – piston rod was analysed. A very good compatibility of both calculation results was achieved. The maximal relative differences did not exceed several percent. It concerned all the evaluated hydrodynamic parameters, like distribution of oil film thickness along the piston rod (Fig. 4) and variations of several parameters versus crank angle: minimum oil gap between the ring and piston rod (Fig. 5), radial ring velocity, hydrodynamic friction force, friction power loss, oil flow rates, scraped oil volumes (Figs. 6, 7) and oil wetted areas of the ring.

Detailed results of the above-described comparisons are presented in report [11].

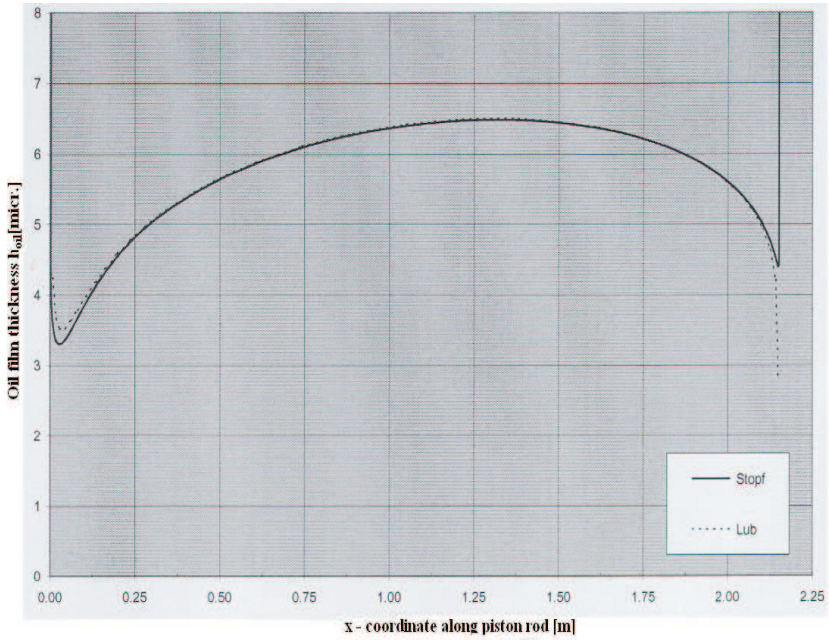

Fig. 4. Comparison of oil film thickness $\mathbf{h}_{oil}$ [μm] distribution along piston rod (or cylinder) calculated by the use of computer programmes STOPF and LUB

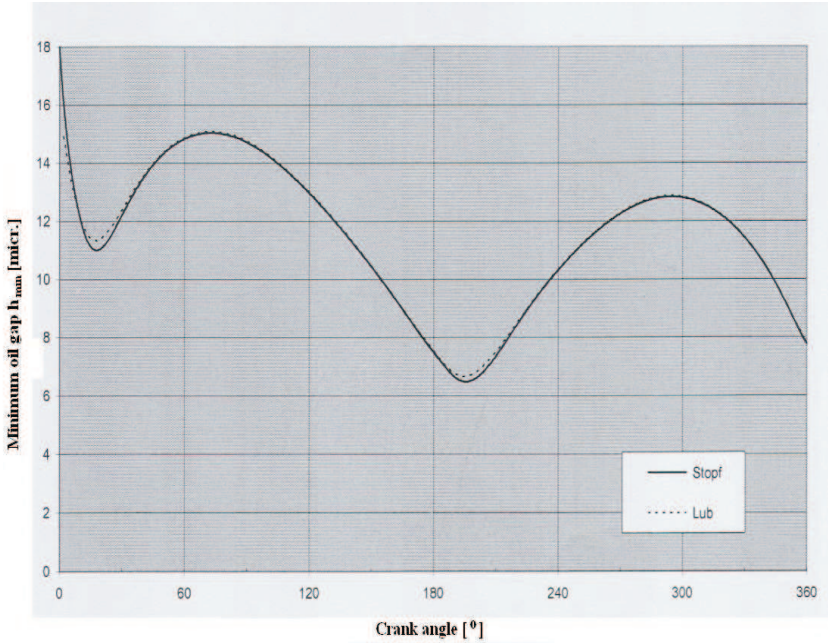

Fig. 5. Comparison of minimum oil gap $\mathbf{h}_{\min}$ [μm] in function of crank angle calculated by the use of computer programmes STOPF and LUB

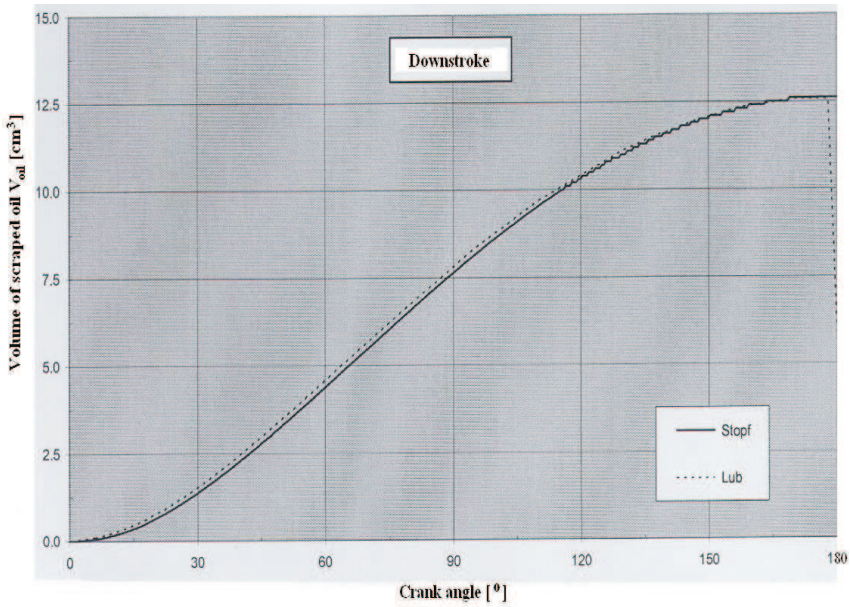

Fig. 6. Comparison of scraped oil volumes $\mathbf{V}_{oil}$ [cm^3] by the ring during downstroke in function of crank angle calculated by the use of computer programmes STOPF and LUB

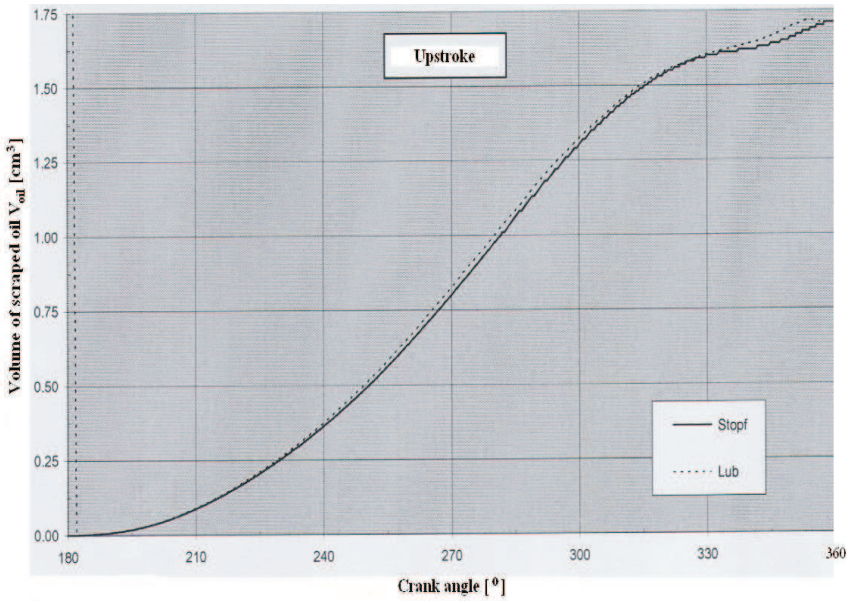

Fig. 7. Comparison of scraped oil volumes $\mathbf{V}_{oil}$ [cm^3] by the ring during upstroke in function of crank angle calculated by the use of computer programmes STOPF and LUB

3.2. Range of experimental investigations determining the basis of verification

A verification of the simulation model has been done by the author for two marine Diesel internal combustion engines. One (of smaller dimensions) was a four-stroke engine and the other was a two-stroke engine. This work was done during the author's several research periods at previously mentioned engine designing centre *Wärtsilä*. According to the request of this company, the types of experimentally tested engines have not been revealed.

In order to carry out the experimental verification of the developed model of gas flow through the labyrinth seal, I applied the measurement results of unsteady gas pressures in cylinder, among piston rings and in crankcase (using piezoelectric sensors mounted in the piston). In addition, for the four-stroke engine, the results of axial movement of rings in piston grooves (applying inductive sensors installed in the piston) and of gas blow-by to crankcase (using a special flow-meter) were accessible [5].

On the other hand, the experimental verification of a hydrodynamic model of piston rings involved measurement results of scraped oil volumes by a gland-box of a two-stroke marine engine. Unfortunately, similar measurements for piston ring packs of tested engines have not been carried out.

3.3. Determination of the set of model parameters

The engine technical data (for instance: main dimensions, rotational speed of maximal power etc.) were taken from the technical documentation that was made available to the author by the engine designing centre *Wärtsilä*. The same situation was in the case of geometrical parameters of the system piston – rings – cylinder. They concerned dimensions of piston rings (including microprofiles of surfaces mating with cylinder liner – for new or worn-out piston rings), chosen mechanical parameters of piston rings (for example: masses, elasticity forces), piston dimensions (including ring grooves), cylinder dimensions (including among other things surface roughness).

Data concerning thermomechanical deformations of piston and cylinder liner (at full engine load) were also made available to the author by the engine designing centre. They concerned calculation results of strength of materials for the mentioned engine parts with the use of finite element method. The wear of cylinder liner (including 1000 hours of engine running) was evaluated on the basis of regularly conducted experimental tests by the engine designing centre *Wärtsilä*. The basic thermodynamic data of the engine (for example: gas pressure and temperature in cylinder and in crankcase, average temperatures of piston rings, thermal state of piston and cylinder surface

etc.) were also made available. These data had been obtained as calculation or experimental results.

In addition, the engine designing company provided information concerning oil quantity for cylinder liner lubrication and physical properties of this oil (for example temperature-dependence of oil viscosity). It has been assumed that oil film temperature along cylinder liner equals calculated temperature distribution on cylinder surface (design data).

A lot of important information has been gathered from the literature [5, 10]. Among other things, it concerned thermodynamic and flow parameters, such as gas flow coefficients through the canals of the labyrinth piston – rings – cylinder, heat transfer coefficients between gas and walls of this labyrinth etc. The final tuning of these parameters values was done by taking into account the known compatibility criteria of numerical calculations and experimental results.

3.4. Compatibility criteria between simulation and experimental results

As the criteria of compatibility between numerical simulation and experimental results, I assumed the below-mentioned parameters [1]. They mainly concern function variations versus crank angle of an internal combustion engine.

a) **Mean square deviation** of measured and calculated function:

$$\sigma = \sqrt{\frac{1}{n}\sum_{i=1}^{n}\left[f_{meas}(x_i) - f_{calc}(x_i)\right]^2} \tag{9}$$

where:

$\boldsymbol{f}_{meas}$ – value of compared function for $\boldsymbol{i}$ – *th* value of argument $\boldsymbol{x}$ (for instance: time $\boldsymbol{t}$, crank angle α, $\boldsymbol{x}$ **-** coordinate along cylinder liner) obtained from measurements,

$\boldsymbol{f}_{calc}$ – value of compared function for $\boldsymbol{i}$ – *th* value of argument $\boldsymbol{x}$ obtained from numerical calculation,

$\boldsymbol{n}$ – number of points of analysed function $\boldsymbol{f}_{meas/calc}\boldsymbol{(x)}$.

b) Extreme values (respectively maximum and minimum) of differences between measured and calculated functions:

$$\Delta f_{\max} = \max_{i=1}^{n}\left[f_{meas}(x_i) - f_{calc}(x_i)\right] \tag{10}$$

$$\Delta f_{\min} = \min_{i=1}^{n}\left[f_{meas}(x_i) - f_{calc}(x_i)\right] \tag{11}$$

c) Extreme values (respectively maximum and minimum) of measured and calculated function:

$$f^{\max}_{meas/calc} = \max_{i=1}^{n} \left[f_{meas/calc}(x_i) \right] \tag{12}$$

$$f^{\min}_{meas/calc} = \min_{i=1}^{n} \left[f_{meas/calc}(x_i) \right] \tag{13}$$

d) Pearson's linear correlation coefficient of measured and calculated function:

$$r_{meas/calc} = \frac{\sum_{i=1}^{n} \left[f_{meas}(x_i) - f^{av}_{meas} \right] \cdot \left[f_{calc}(x_i) - f^{av}_{calc} \right]}{\sqrt{\sum_{i=1}^{n} \left[f_{meas}(x_i) - f^{av}_{meas} \right]^2 \cdot \sum_{i=1}^{n} \left[f_{calc}(x_i) - f^{av}_{calc} \right]^2}} \tag{14}$$

where:

f^{av}_{meas} – average value of measured function; f^{av}_{calc} – average value of calculated function.

3.5. Experimental verification of computational results

3.5.1. Four-stroke Diesel internal combustion engine

The four-stroke marine engine of *Wärtsilä* company was tested as regards gas flow through the labyrinth seal of piston rings. At request of this company, the variations of gas pressure and axial movement of rings in piston grooves are presented as dimensionless parameters ($\boldsymbol{p/p}_{\max}$ and $\boldsymbol{x/x}_{\max}$) related to maximum values (of pressure $\boldsymbol{p}_{\max}$ in cylinder and axial clearance $\boldsymbol{x}_{\max}$ of the ring in a piston groove). Therefore, the values of $\boldsymbol{p}_{\max}$ and $\boldsymbol{x}_{\max}$ are not known for the reader.

Fig. 8 shows a comparison of dimensionless gas pressure $\boldsymbol{p}_3/\boldsymbol{p}_{\max}$ (measured and calculated) for the volume region between piston rings 1 and 2 (Fig. 1a) as a function of crank angle. At the same time, in Tab. 1, appropriate parameters that characterize this comparison are presented. The values of these parameters prove that a satisfactory compatibility of the analysed variation of gas pressure has been achieved. A small discrepancy between the values from measurements and calculations mainly results from simplification assumptions of the model (chapter 2.1) and possible errors of measurements and signal recording.

Then, Fig. 9 shows a comparison of (measured and calculated) relative axial movement $\boldsymbol{x}_1/\boldsymbol{x}_{\max}$ of the first piston ring (compression ring) in the piston groove as a function of crank angle. The chosen parameters that characterize this comparison are presented in Tab. 2. A small time lag between both piston ring movements (measured and calculated) of this piston ring

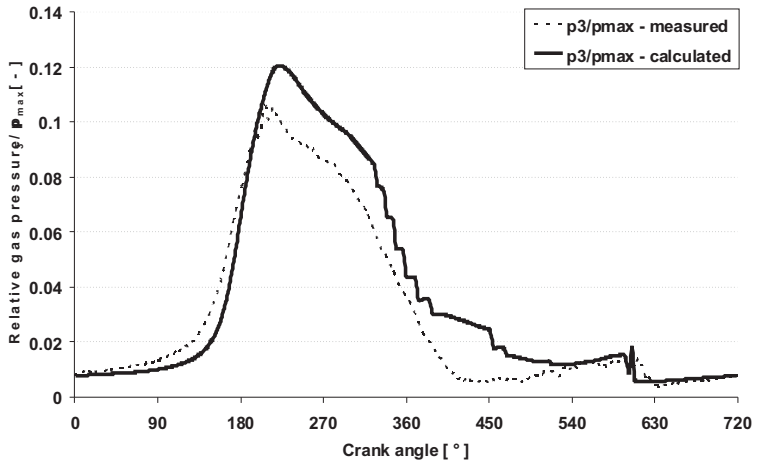

Fig. 8. Comparison of relative gas pressure variation $\boldsymbol{p}_3/\boldsymbol{p}_{\max}$ (measured and calculated) in the volume between the 1^{st} and 2^{nd} piston ring (Fig. 1a) as a function of crankshaft rotation

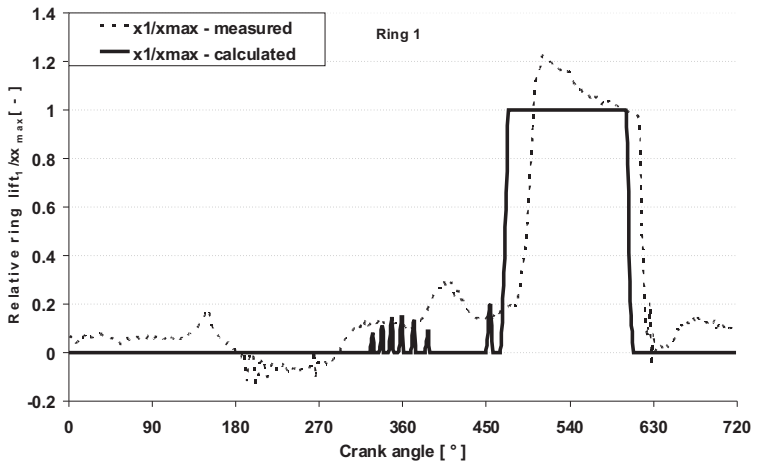

Fig. 9. Comparison of relative ring lift $\boldsymbol{x}_1/\boldsymbol{x}_{\max}$ of the 1^{st} (compression) ring in piston groove (measured and calculated) as a function of crankshaft rotation

is observed. Nevertheless, a satisfactory qualitative compatibility of both compared functions has been achieved.

However, the measurement result shows a certain inaccuracy. In the case of the piston ring jumping to the upper shelf of piston groove, the relative lift $\boldsymbol{x}_1/\boldsymbol{x}_{\max}$ of the ring shortly exceeds the value 1. In addition, when coming back to the lower shelf of piston groove, the relative lift of the ring is lower than 0. It proves that the nominal axial clearance of the ring in piston groove is exceeded. The possible reason for this fact might be the measurement

inaccuracy, which results from difficulties in determining the ring movement during the reciprocating motion of the piston.

Table 1.
Compatibility of relative gas pressure variation $\mathbf{p_3/p_{max}}$ (measured and calculated)

Relative difference between maximal values (measured and calculated) [%]	Quotient of average values (of calculated and measured results) [–]	Quotient of mean square deviation to measured maximal value [%]	Linear correlation coefficient of Pearson (of measured and calculated results) [–]
13.6	**1.18**	**10.77**	**0.98**

Table 2.
Compatibility of relative ring lift $\mathbf{x_1/x_{max}}$ in piston groove (measured and calculated)

Quotient of average values (of calculated and measured results) [–]	Pearson's correlation coefficient (of measured and calculated results) [–]
0.75	**0.86**

The next compared parameter is a gas blow-by through the labyrinth seal of piston rings into the engine crankcase. In Tab. 3 the measured and calculated exhaust gas blow-by and the quotient of the calculated to measured value are given. A very good compatibility of both results has been achieved.

Table 3.
Compatibility of gas blow-by to the engine crankcase (measured and calculated)

Measured value [dm^3/min]	Calculated value [dm^3/min]	Quotient of calculated and measured value [–]
83.1	**82.2**	**0.989**

3.5.2. Two-stroke Diesel internal combustion engine

The test object was a turbocharged two-stroke marine Diesel engine designed by *Wärtsilä* company [2, 8]. This engine had two seal systems that were included for experimental verification:

a) labyrinth seal of piston rings,
b) pack of seal and scraper rings making a gland-box that separates the piston underside from crankcase of the engine.

Variations of gas pressure between piston rings

The piston of this engine has four one-lip piston rings. In this case, the gas flow model is more complicated than that applied for the four-stroke engine (having only three piston rings).

Fig. 10 shows a comparison of measured and calculated dimensionless gas pressures $\boldsymbol{p_i/p_{max}}$ (i = 1, 3, 5, 7) for the main volume regions of the

labyrinth seal (Fig. 1b) as a function of crank angle. The presented results concern a full engine load. In Tab. 4 the appropriate parameters that characterize this comparison are presented. A satisfactory qualitative and quantitative compatibility of the analysed pressure variations has been achieved. In case of this engine axial movements of rings in piston grooves have not been measured.

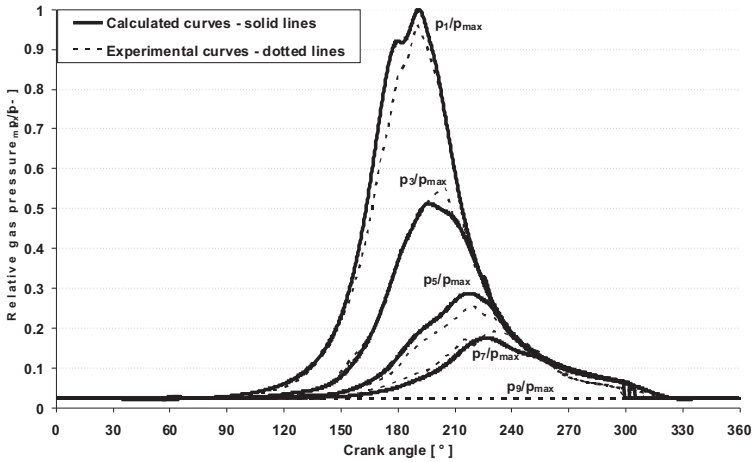

Fig. 10. Comparison of relative gas pressure variations $\boldsymbol{p}_i/\boldsymbol{p}_{\max}$ (measured and calculated) as a function of crankshaft rotation. Gas pressure nomenclature: $\boldsymbol{p}_1$ – in combustion chamber, $\boldsymbol{p}_3$ – between the 1^{st} and 2^{nd} piston ring, $\boldsymbol{p}_5$ – between the 2^{st} and 3^{rd} piston ring, $\boldsymbol{p}_7$ – between the 3^{rd} and 4^{th} piston ring, $\boldsymbol{p}_9$ – under the piston

Table 4.

Compatibility of gas pressure variations (measured and calculated)

Evaluated variations of relative gas pressures	Relative difference between maximal values (measured and calculated) [%]	Quotient of average values (of calculated and measured results) [–]	Quotient of mean square deviation to measured maximal value [%]	Pearson's correlation coefficient (of measured and calculated results) [–]
$\mathbf{p_1/p_{max\,1}}$	**-3.80**	**1.077**	**3.20**	**0.997**
$\mathbf{p_3/p_{max\,1}}$	**7.20**	**1.012**	**1.94**	**0.998**
$\mathbf{p_5/p_{max\,1}}$	**-12.13**	**1.118**	**5.85**	**0.994**
$\mathbf{p_7/p_{max\,1}}$	**9.07**	**0.962**	**5.74**	**0.981**

Volumes of scraped oil by gland-box of marine engine

The purpose of a gland-box is to separate the piston underside as tight as possible from the crankcase. The engine designing centre *Wärtsilä* made

available to the author measurement results of scraped oil volumes by the gland-box of a chosen engine. Special oil tanks were installed in the tested engine, where lubricating oil flew in. Then, oil volumes scraped up to piston underside and down to crankcase during 24 hours of engine running were measured.

One of many input parameters of the simulation programme is the velocity of oil fog deposition on a free surface of piston rod. This parameter has been chosen in such a way that a good compatibility between measured and calculated oil volumes scraped down into crankcase has been achieved. In Tab. 5, a comparison of measured and calculated parameters and a percent scatter of results are given.

Table 5.
Compatibility of the scraped oil quantities (measured and calculated) by the gland-box

Analyzed volumes of lubricating oil	Average value of measured parameter [dm^3/24h]	Calculated value [dm^3/24h]	Relative difference between measured and calculated value [%]
Quantity scraped to piston underside	**8**	**7.252**	**9.35**
Quantity scraped to crankcase	**12000**	**11020**	**8.17**

4. Conclusions

1. The developed mathematical model and simulation programme have been experimentally verified for two marine engines (during working periods at the engine designing centre *Wärtsilä* in Switzerland);
2. The simulation model characterizes well the piston ring pack operation of different kinds of internal combustion engines (two- and four-stroke). It concerns mainly variations of gas pressure among the rings as functions of crank angle and exhaust gas flow rates (blow-by) through the labyrinth seal of a piston ring pack;
3. In case of axial movements of piston rings in piston grooves, a greater discrepancy between the results of calculations and experimental investigations can be noticed. A small time-lag between calculated and measured piston ring movements is observed. In addition, the measurement results show a certain inaccuracy that consists in exceeding the nominal axial clearance of the ring in piston groove. The possible reason for this fact is inaccuracy of the measurement, which results from difficulties of determining piston rings movements during the reciprocating motion of the piston;

4. Analyzing scraped oil volumes by the ring pack (of the gland-box of marine internal combustion engine), we can notice a satisfactory quantitative compatibility of results concerning numerical calculations and experimental investigations.

Manuscript received by Editorial Board, December 11, 2008;
final version, April 20, 2009.

REFERENCES

[1] Bobrowski D.: Probabilistyka w zastosowaniach technicznych, WNT, Warszawa 1980.
[2] Demmerle R., Barrow S., Terrettaz F., Jaquet D.: New Insights into the Piston Running Behaviour of "Sulzer" Large Bore Diesel Engines, CIMAC Congress, Hamburg May 2001.
[3] Greenwood J., Tripp J.H.: The contact of Two Nominally Flat Rough Surfaces, Proc I. Mech. E., Vol. 185, pp. 625-633, 1971.
[4] Iskra A.: Parametry filmu olejowego w węzłach mechanizmu tłokowo – korbowego silnika spalinowego, Wydawnictwo Politechniki Poznańskiej, Poznań 2001.
[5] Koszałka G.: Modelling the blowby in internal combustion engine, Part 1: A mathematical model, The Archive of Mechanical Engineering, Vol. LI, Number 2, p. 245-257, 2004; Part 2: Primary calculations and Verification of the model, The Archive of Mechanical Engineering, Vol. LI, No. 4, p. 595-607, 2004.
[6] Patir N., Cheng H.S.: An Average Flow Model for Determining Effects of Three-Dimensional Roughness on Partial Hydrodynamic Lubrication, Transactions of ASME, Vol 100, January 1978.
[7] Patir N., Cheng H.S.: Application of Average Flow Model to Lubrication Between Rough Sliding Surfaces, Transactions of ASME, Vol 101, April 1979.
[8] Räss K., Amoser M.: Progressive development of two-stroke engine tribology, Paper No. 83, CIMAC Congress, Vienna 2007.
[9] Serdecki W.: Badania współpracy elementów układu tłokowo – cylindrowego silnika spalinowego, Wydawnictwo Politechniki Poznańskiej, Poznań, 2002.
[10] Tian T., Nordzij L.B., Wong V.W., Heywood J.B.: Modeling Piston-Ring Dynamics, Blowby, and Ring-Twist Effects, Transactions of ASME, Journal of Engineering for Gas Turbines and Power, Vol. 120, p. 843-854, October 1998.
[11] Wolff A.: Verifikation des erstellten Computerprogramms STOPF. Vergleich der Berechnungs ergebnisse des Programms STOPF und des Programms LUB für die Hydrodynamik der Kolbenringe, report of marine engines designing centre Wärtsilä, Winterthur, 2000.
[12] Wolff A., Piechna J.: Numerical simulation of piston ring pack operation, The Archive of Mechanical Engineering, Vol. L, No. 3, p. 303- 329, 2003.
[13] Wolff A., Piechna J.: Numerical simulation of piston ring pack operation in the case of mixed lubrication, The Archive of Mechanical Engineering, Vol. LII, No. 3, p. 157-190, 2005.
[14] Wolff A.: Badania symulacyjne przepływu gazu przez uszczelnienie labiryntowe pierścieni tłokowych, Zeszyty Naukowe Instytutu Pojazdów, Wydział Samochodów i Maszyn Roboczych, Politechnika Warszawska, zeszyt 2, str. 39-65, Warszawa 2007.
[15] Wolff A., Piechna J.: Numerical simulation of piston ring pack operation with regard to ring twist effects, The Archive of Mechanical Engineering, Vol. LIV, No. 1, p. 65-99, Warsaw 2007.

[16] Wolff A.: Symulacja cyfrowa działania pakietu pierścieni tłokowych, Polska Akademia Nauk Oddział w Krakowie, Teka Komisji Motoryzacji pt. "Konstrukcja, badania, eksploatacja, technologia pojazdów samochodowych i silników spalinowych", zeszyt nr 33-34, str. 467-474, Kraków 2008 r.

Weryfikacja eksperymentalna modelu funkcjonowania pakietu pierścieni tłokowych silnika spalinowego

Streszczenie

W artykule przedstawiono kompleksowy model ruchu pakietu pierścieni tłokowych po filmie olejowym o grubości porównywalnej z sumaryczną chropowatością pierścieni i gładzi cylindrowej. Zaadaptowano [13] model przepływu oleju w szczelinie o chropowatych ściankach Patira i Chenga [3, 4] oraz model elastycznego kontaktu chropowatych powierzchni Greenwooda i Trippa [1]. Opracowano także model przepływu gazu przez uszczelnienie labiryntowe pierścieni [14,16], jak i model odkształceń kątowych pierścieni i ich pionowych przeskoków w rowkach tłoka [15,16].

W odróżnieniu od poprzednich artykułów autora, przedstawiono eksperymentalną weryfikację głównych członów opracowanego kompleksowego modelu matematycznego oraz oprogramowania. Uzyskano relatywnie dobrą zgodność ilościową i jakościową wyników obliczeń symulacyjnych i badań eksperymentalnych.